

# H<sub>2</sub>S treatment improves the protective effect of mesenchymal stem cell-derived exosomes on renal ischemia/reperfusion fibrosis by suppressing inflammatory signaling of TGF- $\beta$ and NF- $\kappa$ B as well as radical oxygen species generation

Ya-Peng Wang<sup>1</sup>, Rui-Xiao Wang<sup>2</sup>, Zhao-Jun Li<sup>1</sup>, Xue-Yi Wang<sup>3</sup>, Xia Qiao<sup>4</sup>, Tao Ma<sup>5</sup>, Zong-Ying Jiang<sup>2</sup>, Ling-Ya Huang<sup>2</sup>

<sup>1</sup>School of Nursing, Ningxia Medical University, Yinchuan, Ningxia, China

<sup>2</sup>Department of Pathology, General Hospital of Ningxia Medical University, Yinchuan, Ningxia, China

<sup>3</sup>Yinchuan Hospital of Traditional Chinese Medicine, Yinchuan, Ningxia, China

<sup>4</sup>Ningxia Key Laboratory of Clinical and Pathogenic Microbiology, General Hospital of Ningxia Medical University, Yinchuan, Ningxia, China

<sup>5</sup>The Third Department of Surgical Oncology, General Hospital of Ningxia Medical University, Yinchuan, Ningxia, China

## Corresponding author:

Ling-Ya Huang  
Department of Pathology  
General Hospital of Ningxia  
Medical University  
804 Shengli Street, Yinchuan  
Ningxia, 750004, China  
E-mail: molemal@yeah.net

**Submitted:** 19 June 2021; **Accepted:** 26 September 2021

**Online publication:** 29 October 2021

Arch Med Sci

DOI: <https://doi.org/10.5114/aoms/142601>

Copyright © 2021 Termedia & Banach

## Abstract

**Introduction:** Hydrogen sulfide (H<sub>2</sub>S) has been reported to regulate signaling pathways responsible for development of renal ischemia/reperfusion (I/R) associated fibrosis. In this study, we hypothesized that preconditioning with H<sub>2</sub>S may boost the protective effect of mesenchymal stem cells- (MSC) -derived exosomes (EXOs) on renal I/R fibrosis.

**Material and methods:** Real-time polymerase chain reaction (PCR) and Western blot were performed to evaluate mRNA and protein expression of Nrf2, NF- $\kappa$ B, TGF- $\beta$ ,  $\alpha$ -SMA, and collagen type II (Col2). H & E and Masson staining were carried out to examine the kidney injury and fibrosis in rats.

**Results:** H<sub>2</sub>S-preconditioned EXOs substantially promoted the protective effect of EXOs on the development of kidney injury as well as associated fibrosis in I/R rats. EXO treatment significantly restored the activated gene and protein expression of NF- $\kappa$ B, TGF- $\beta$ ,  $\alpha$ -SMA, and Col2 in I/R rats and the cellular model of hypoxia/reoxygenation (H/R), while H<sub>2</sub>S preconditioning remarkably strengthened this effect of EXOs. Additionally, H<sub>2</sub>S preconditioning remarkably strengthened the efficiency of EXOs in restoring the activated expression of IL-1 $\alpha$ , IL-6, IL-12 and TNF- $\alpha$  as well as altered activities of superoxide dismutase (SOD), malondialdehyde (MDA), H<sub>2</sub>O<sub>2</sub>, glutathione S-transferase (GST) and glutathione peroxidase (GPx) in I/R rats and the cellular model of H/R.

**Conclusions:** This study utilized I/R rats to demonstrate that the effect of H<sub>2</sub>S-preconditioned exosomes in suppressing inflammation and radical oxygen species (ROS) generation was better than that of unconditioned exosomes. To be specific, exosomes, especially H<sub>2</sub>S-preconditioned exosomes, could not only reduce the expression of NF- $\kappa$ B and the downstream inflammatory responses, but also promote the expression of Nrf2 and inhibit ROS generation, which explained the molecular mechanism underlying the protective effect of H<sub>2</sub>S-preconditioned exosomes on renal I/R associated fibrosis.

**Key words:** H<sub>2</sub>S, MSC, exosomes, renal ischemia, reperfusion, fibrosis, inflammation, ROS.

## Introduction

Fibrosis is a pathophysiological condition that develops following renal ischemia-reperfusion (I/R) injury, and it is a very common medical condition worldwide [1]. I/R produces a microenvironment in kidney tissues which lacks oxygen and necessary nutrients, leading to an increase in oxidative stress and production of radical oxygen species (ROS). These conditions cause cell apoptosis, necrosis and injury in the interstitial cells of the kidney [2, 3]. The immune response generated within the renal interstitium activates mesangial cell proliferation and extracellular matrix production, causing chronic renal injury and fibrosis. As a result, blood capillaries in the interstitium layer become smaller and produce an aggressive reaction like anoxia, further worsening the kidney injury [4–6]. The I/R condition impacts the process of oxidative phosphorylation, causing increased levels of reactive oxygen species. Therefore, antioxidants have been shown to attenuate progression of I/R related kidney injury [7].

Previous studies have explored the beneficial effects of mesenchymal stem cells (MSCs) in various pathophysiological conditions, such as heart disease, stroke, and autoimmune disease [8, 9]. Considering the ability of the MSCs to differentiate into other tissues, it was believed that the injured kidney tissues can be regenerated [10, 11]. Microvesicles, also called exosomes (EXOs) (30–100 nm), are usually extracted from various body fluids and supernatant layers of cell culture [12–14]. Exosomes contain a complex cocktail of components ranging from different types of proteins, genetic material such as RNA, lipids and enzymes. Exosomes function as an effective method of cell-cell communication [14, 15].

Protective effects of in situ synthesized gaseous molecules, also known as gasotransmitters, against tissue ischemia-reperfusion injury (IRI) have been reported recently. The list of recently discovered gasotransmitters includes nitric oxide (NO), carbon monoxide (CO), and the latest member is hydrogen sulfide ( $H_2S$ ) [16, 17]. The protection offered by  $H_2S$  against renal injury has been shown in various models, including brain, intestine, liver lung and heart. The proposed mechanism of action of the protective effect of  $H_2S$  involves antiapoptotic, antioxidant and anti-inflammatory effects [18, 19]. The effects of exogenous  $H_2S$  treatment on the acute recovery period needed to reduce inflammation in I/R rat models were investigated in the current study [20].

A complex signaling pathway is responsible for anti-inflammatory effects of  $H_2S$ . The majority of inflammatory responses involved NF- $\kappa$ B as an intracellular signaling mediator [21]. It was also shown that, upon  $H_2S$  treatment, the treated cells

switched into a reversible hypometabolic and hibernation-like state. The hypothesized hypometabolism induced by  $H_2S$  treatment functions by lowering the mitochondrial activity via binding reversibly to cytochrome c oxidase. During hypometabolism, animals are protected from hypoxia and their organs from I/R due to a lack of oxygen demand. Administration of  $H_2S$  not only scavenges reactive species, such as ROS or reactive nitrogen species (RNS), but also produces glutathione, a natural antioxidant. Overall,  $H_2S$  acts as a protective agent in animal models with renal injury [22].

Hypoxia-preconditioned MSCs have been proved to be an effective cell therapy method to prevent renal fibrosis and inflammation [23]. Also  $H_2S$  has been reported to participate in renal I/R fibrosis-associated signaling pathways in recent studies [22, 24, 25]. In this study, we hypothesized that preconditioning with  $H_2S$  could boost the effect of EXOs in the therapy of renal I/R fibrosis. By establishing an I/R rat model, we aimed to investigate the potential therapeutic effect of  $H_2S$ -preconditioned EXOs and underlying mechanisms on renal I/R fibrosis.

## Material and methods

### Animal and treatment

Male SD rats with age ranging between six and eight weeks were maintained at room temperature. Bone marrow was collected from the rats at six weeks, whereas the I/R model was generated using eight-week-old rats. The animal studies were performed according to an IACUC approved protocol. The renal ischemia reperfusion injury model was set up by carefully harnessing the unilateral renal artery. Before the surgery, the rats were given an intraperitoneal injection of a mixture of anesthetics. The left kidneys of the rats were exposed following the procedure of laparotomy. Using a vascular clamp, the renal pedicle was clamped for 1 h. Later, the reperfusion procedure was carried out. Animals were divided into four groups with 12 animals in each group, i.e., 1) the control group (a group of animals without any treatments), 2) the I/R group (animals were subjected to the surgery described before to make the IRI model), 3) the EXOs group (animals were treated with 100  $\mu$ g of exosomes without  $H_2S$  treatment) and 4) EXOs with  $H_2S$  group (animals were treated with  $H_2S$  and pretreated 100  $\mu$ g of EXOs). The institutional animal ethics committee has approved the protocols of this study.

### Preparation of mesenchymal stem cells

Following a procedure described in a previous publication [26], marrow from bones was collected from the rats. The bone marrow cells were cultured

in DMEM (Sigma-Aldrich, St. Louis, MO, USA) with 10% FBS (Sigma-Aldrich). The cells were grown in four phases and used as rat MSCs for transplantation. According to instructions from a previous publication [27], NaHS (Sigma-Aldrich Chemical, St. Louis, MO, USA) was prepared at a concentration of 10  $\mu$ mol/ml, and then the MSCs were pre-conditioned with 200  $\mu$ mol/l NaHS for 30 min.

#### Measurement of carbon monoxide production in kidney

Kidney samples were homogenized and centrifuged to collect the protein content from the supernatant. The production of CO in kidney samples was measured by gas chromatography-mass spectroscopy following instructions in previous publications [28].

#### Measurement of nitric oxide production in kidney

The NO production was determined in urine using a colorimetry assay kit (Cayman Chemical; Ann Arbor, CA, USA) following the instructions of the manufacturer.

#### Real-time PCR

To explore the effect of H<sub>2</sub>S treated exosomes, the assays were carried out to analyze the expression of Nrf2, NF- $\kappa$ B, TGF- $\beta$ ,  $\alpha$ -SMA, and Col2 in I/R rat models and HK-2 cells. To carry out the measurements, the intact RNA was initially obtained from each sample by utilizing an RNAiso Plus RNA extraction reagent (Thermo Fisher, MA) using the provided protocol. Then, the isolated RNA from each sample was reverse transcribed into cDNA templates using a TaqMan Advanced cDNA Synthesis kit (Thermo Fisher Scientific, Waltham, MA) along with a QuantiTect Reverse Transcription Kit (Qiagen, MD) following the specific assay procedure received with the kit. Then, quantitative real-time PCR was performed using a Fast Start Universal SYBR Green Master Mix assay kit (Roche, Basel, Switzerland) following the specific assay procedure received with the kit. The real-time PCR reaction was done on an ABI Prism 7900HT real-time PCR machine (Applied Biosystems, Foster City, CA) using U6 as well as GAPDH as the internal control for the normalization of measured relative expression of target genes, i.e., Nrf2, NF- $\kappa$ B, TGF- $\beta$ ,  $\alpha$ -SMA, and Col2.

#### Western blot analysis

The total protein content was extracted from each sample by making use of a radio immunoprecipitation assay kit (Abcam, CA) following the specific assay procedure received with the kit. Then, 50  $\mu$ g of each protein sample was resolved

using SDS-PAGE and blotted onto polyvinylidene fluoride (PVDF) membranes, which were then blocked using 5% skimmed milk at ambient temperature for 1 h before they were incubated for 24 h at 4°C with corresponding primary antibodies of Nrf2, NF- $\kappa$ B, TGF- $\beta$ ,  $\alpha$ -SMA, Col2 (Abcam, Cambridge, MA) followed by incubation with suitable HRP-conjugated secondary antibodies for 1 h at room temperature in accordance with the specific instructions provided by the antibody manufacturer. After color development using an enhanced chemiluminescence (ECL) assay kit (Amersham Pharmacia, Piscataway, NJ) following the specific assay procedure received with the kit, the relative protein expression of catechol-O-methyltransferase (COMT) in each sample was determined using a Bio-Rad imaging system (Bio-Rad Laboratories, Hercules, CA) in accordance with the instructions provided by the machine manufacturer.

#### H & E staining

The tissue samples were fixated with formalin and embedded with paraffin to stain with H & E stain. The sections were observed using a fluorescence microscope.

#### Masson staining

The tissue samples were fixated with formalin, deparaffinized, and rehydrated with 100% alcohol, 95% alcohol and 75% alcohol. The tissue samples were re-fixed in Bouin's solution for 60 min at 56°C and rinsed with running tap water. Later, they were stained in Weigert's iron hematoxylin for a few minutes and again washed with water. Immediately after this, Biebrich scarlet-acid fuchsin solution was applied on the tissue samples for ten minutes. Then they were rinsed with water and restained with phosphomolybdic-phosphotungstic acid solution for ten minutes.

#### Enzyme-linked immunosorbent assays

Enzyme-linked immunosorbent assays (ELISA) were performed to measure IL-1 $\alpha$ , IL-6, IL-12 and TNF- $\alpha$  levels using commercial kits (Abcam, Cambridge, MA). Samples at 1/10 dilution were tested for IL-1 $\alpha$ , IL-6, IL-12 and TNF- $\alpha$  according to the manufacturer's instructions.

#### Cell culture

The human renal proximal tubular epithelial cell line human kidney-2 (HK-2) was obtained from American Type Culture Collection (Manassas, VA, USA). The cell lines were preserved in RPMI-1640 medium supplied with 10% fetal bovine serum (FBS) (Thermo Fisher Scientific, Waltham, MA), and put in an incubator at 37°C with 5% CO<sub>2</sub>. HK-2

cells were divided into four groups, i.e., 1) control group (HK-2 cells without any treatments); 2) hypoxia/reoxygenation (H/R) group (HK-2 cells were put in hypoxic conditions, i.e., 37°C, 1% O<sub>2</sub>, 94% N<sub>2</sub> and 5% CO<sub>2</sub> for 12 h in glucose- and serum-free medium to induce hypoxic injury. Later, the cells were placed in normal condition (5% CO<sub>2</sub>) for reoxygenation for 12 and 24 hours; 3) EXOs group (HK-2 cells were treated with exosomes without H<sub>2</sub>S treatment); and 4) EXOs with H<sub>2</sub>S group (HK-2 cells were treated with the H<sub>2</sub>S pretreated exosomes). As per the manufacturer's protocols, the HK-2 cells were transfected using Lipofectamine 2000 (Thermo Fisher Scientific, Waltham, MA).

### Enzyme assays

The HK-2 cells were lysed to analyze the levels of malondialdehyde (MDA) and superoxide dismutase (SOD) activity. The corresponding assay kits were used to this end following the protocols provided by the manufacturer. The HK-2 cells were cultured in DMEM medium plus fetal bovine serum. To determine the amount of hydrogen peroxide present in the kidney tissues, the kidney extracted from the animals was perfused and homogenized. Later, the reagent, containing 10 U/mL horseradish peroxidase, was added to the homogenized tissues according to the provider's assay protocol. Then, the reading from the fluorescence instrument was analyzed. To detect the enzyme activity in the extracted kidney samples, the adduct of GSH and CDNB was detected at 340 nm. To measure the SOD and glutathione peroxidase (GPx) activity, an indirect method of detecting reduction of NBT by the enzyme xanthine-xanthine oxidase was used as described previously [16].

### Statistical analysis

All outcomes were expressed as mean ± standard deviations. The statistical significance of in-

ter-group differences was evaluated by Student's *t*-test. The statistical analyses were performed using Prism 7.0 software (GraphPad, La Jolla, CA). Value of *p* < 0.05 was considered to represent statistical significance.

## Results

### H<sub>2</sub>S-preconditioned EXOs effectively restored the kidney function impairment in I/R rat models

MSCs were pretreated with H<sub>2</sub>S followed by EXO collection. Electron microscope analysis indicated no obvious difference between EXOs collected from H<sub>2</sub>S preconditioned MSCs and untreated MSCs (Figure 1 A). Western blot was performed to analyze the surface markers CD63, CD69 and CD81 on EXOs collected from H<sub>2</sub>S preconditioned MSCs and untreated MSCs; no significant difference was found (Figure 1 B). An I/R rat model was established and subjected to EXO treatment. H&E staining analysis indicated that the kidney injury was remarkably elevated in I/R rat models. EXOs treatment notably decreased the kidney injury; moreover, EXOs from H<sub>2</sub>S preconditioned MSCs showed a reinforced efficiency in attenuating the kidney injury in I/R rat models (Figure 1 C). Furthermore, Masson staining was performed to evaluate the kidney fibrosis in I/R rats under distinct conditions. H<sub>2</sub>S-preconditioned EXOs apparently maintained the kidney fibrosis in I/R rats (Figure 1 D). Additionally, the increased kidney functional parameters SCr (Figure 1 E) and BUN (Figure 1 F) were also effectively restored by H<sub>2</sub>S-preconditioned EXOs. Moreover, it was found that H<sub>2</sub>S preconditioning reinforced the efficiency of EXOs in suppressing NO production in I/R rats (Figure 1 G), while the CO production was not influenced by these treatments (Figure 1 H).

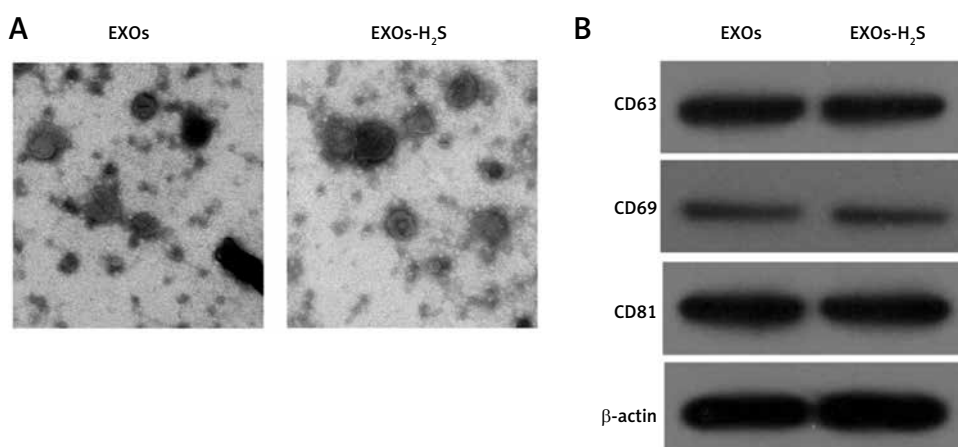


**Figure 1.** H<sub>2</sub>S-preconditioned EXOs effectively restored the kidney function impairment in I/R rat models. **A** – Microscope examination of EXOs isolated from MSCs and H<sub>2</sub>S-preconditioned MSCs. **B** – Western blot analysis of CD63, CD69 and CD81 in EXOs isolated from MSCs and H<sub>2</sub>S-preconditioned MSCs



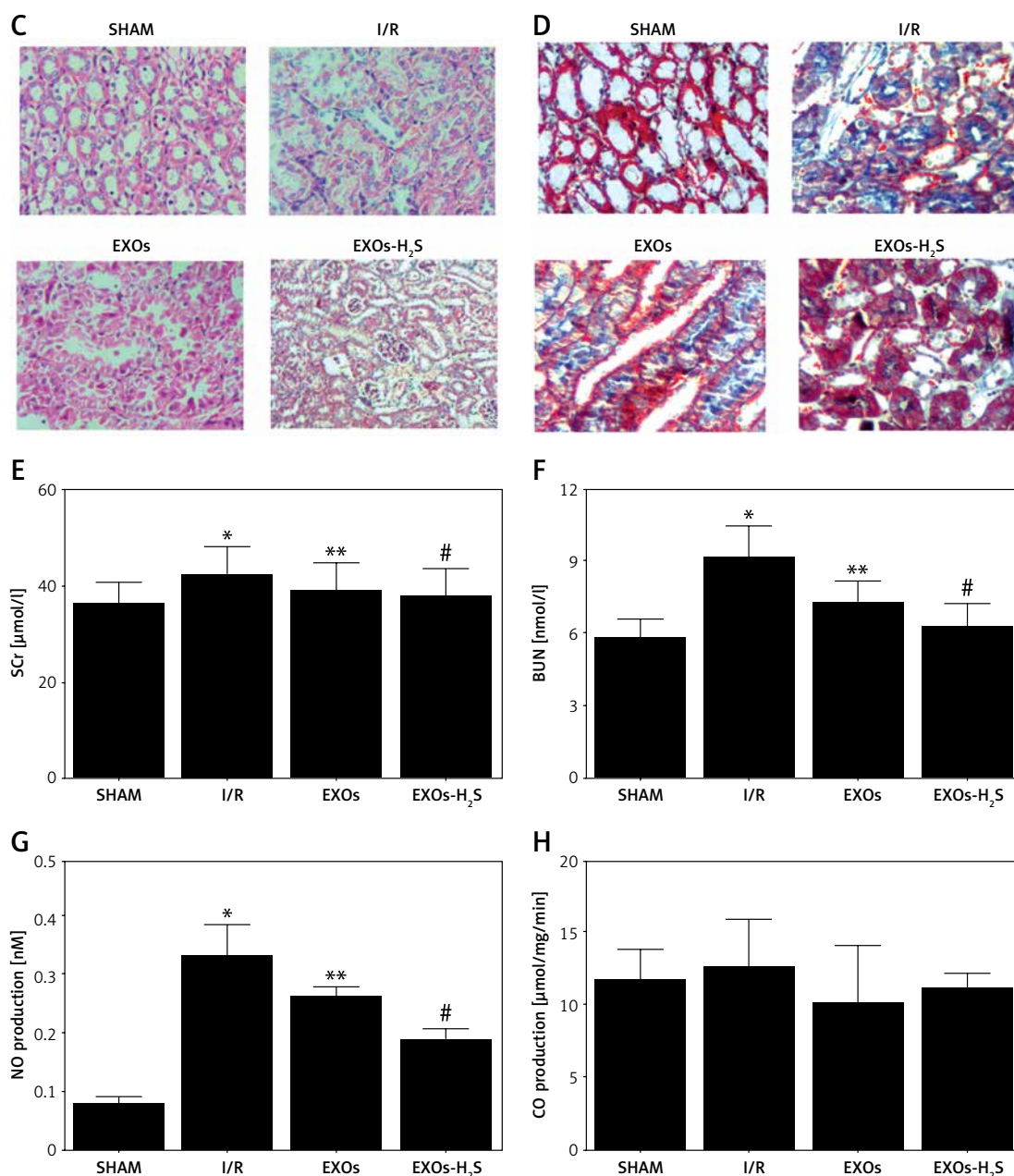


**Figure 1.** Cont. **C** – H & E staining indicated that H<sub>2</sub>S preconditioning reinforced the efficiency of EXOs in restoring kidney injury in I/R rats. **D** – Masson staining indicated that H<sub>2</sub>S preconditioning reinforced the efficiency of EXOs in restoring kidney fibrosis in I/R rats. **E** – H<sub>2</sub>S preconditioning reinforced the efficiency of EXOs in restoring the SCr in I/R rats (\* $p$  < 0.05 vs. SHAM group; \*\* $p$  < 0.05 vs. I/R group; # $p$  < 0.05 vs. EXOs group). **F** – H<sub>2</sub>S preconditioning reinforced the efficiency of EXOs in restoring the BUN in I/R rats (\* $p$  < 0.05 vs. SHAM group; \*\* $p$  < 0.05 vs. I/R group; # $p$  < 0.05 vs. EXOs group). **G** – H<sub>2</sub>S preconditioning reinforced the efficiency of EXOs in suppressing NO production in I/R rats (\* $p$  < 0.05 vs. SHAM group; \*\* $p$  < 0.05 vs. I/R group; # $p$  < 0.05 vs. EXOs group). **H** – The CO production was comparable between all rat animal groups

### H<sub>2</sub>S-preconditioned EXOs effectively restored the expression of NF- $\kappa$ B, TGF- $\beta$ , $\alpha$ -SMA, and Col2 protein in I/R rats

Western blot was carried out to analyze the expression of Nrf2, NF- $\kappa$ B, TGF- $\beta$ ,  $\alpha$ -SMA, and Col2 in I/R rats under distinct conditions (Figure 2 A). The expression of Nrf2 was notably elevated in I/R rats compared with the control. EXO treatment further

increased the Nrf2 expression and H<sub>2</sub>S-preconditioned EXOs showed higher efficiency in enhancing the Nrf2 expression in I/R rats (Figure 2 B). Even though the expression of NF- $\kappa$ B, TGF- $\beta$ ,  $\alpha$ -SMA, and Col2 in I/R rats was remarkably increased, EXO treatment effectively attenuated the up-regulation of NF- $\kappa$ B, TGF- $\beta$ ,  $\alpha$ -SMA and Col2 in I/R rats. H<sub>2</sub>S preconditioning further decreased the elevated expression of NF- $\kappa$ B (Figure 2 C),

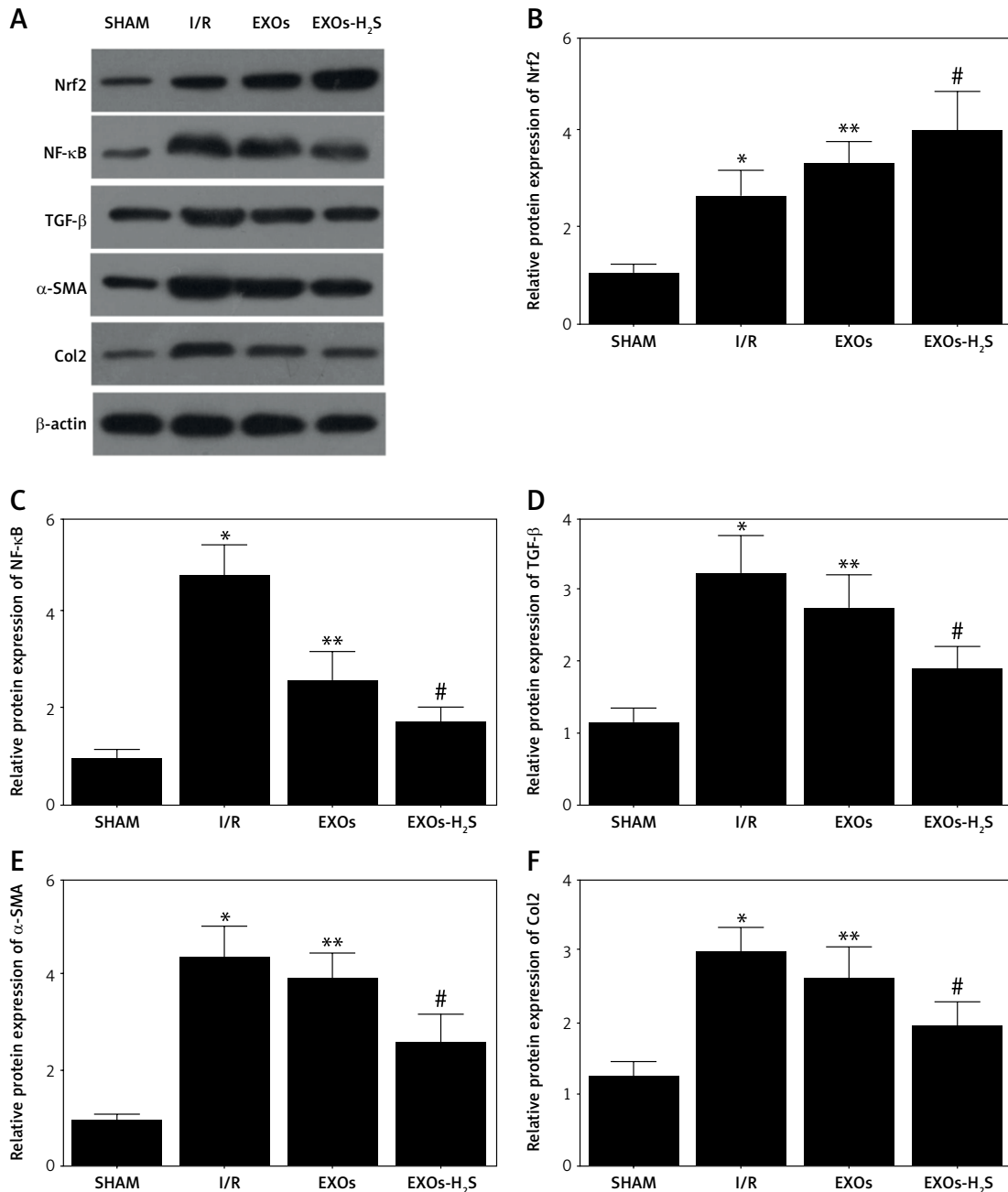


**Figure 2.** H<sub>2</sub>S-preconditioned EXOs effectively restored the expression of NF-κB, TGF-β, α-SMA, Col2 protein in I/R rats. **A** – Western blot analysis of Nrf2, NF-κB, TGF-β, α-SMA, Col2 protein in I/R rats under distinct conditions. **B** – H<sub>2</sub>S-preconditioned EXOs further increased the protein expression of Nrf2 in I/R rats (\**p* < 0.05 vs. SHAM group; \*\**p* < 0.05 vs. I/R group; #*p* < 0.05 vs. EXOs group). **C** – H<sub>2</sub>S-preconditioned EXOs effectively restored the protein expression of NF-κB protein in I/R rats (\**p* < 0.05 vs. SHAM group; \*\**p* < 0.05 vs. I/R group; #*p* < 0.05 vs. EXOs group). **D** – H<sub>2</sub>S-preconditioned EXOs effectively restored the protein expression of TGF-β protein in I/R rats (\**p* < 0.05 vs. SHAM group; \*\**p* < 0.05 vs. I/R group; #*p* < 0.05 vs. EXOs group). **E** – H<sub>2</sub>S-preconditioned EXOs effectively restored the protein expression of α-SMA protein in I/R rats (\**p* < 0.05 vs. SHAM group; \*\**p* < 0.05 vs. I/R group; #*p* < 0.05 vs. EXOs group). **F** – H<sub>2</sub>S-preconditioned EXOs effectively restored the protein expression of Col2 protein in I/R rats (\**p* < 0.05 vs. SHAM group; \*\**p* < 0.05 vs. I/R group; #*p* < 0.05 vs. EXOs group).

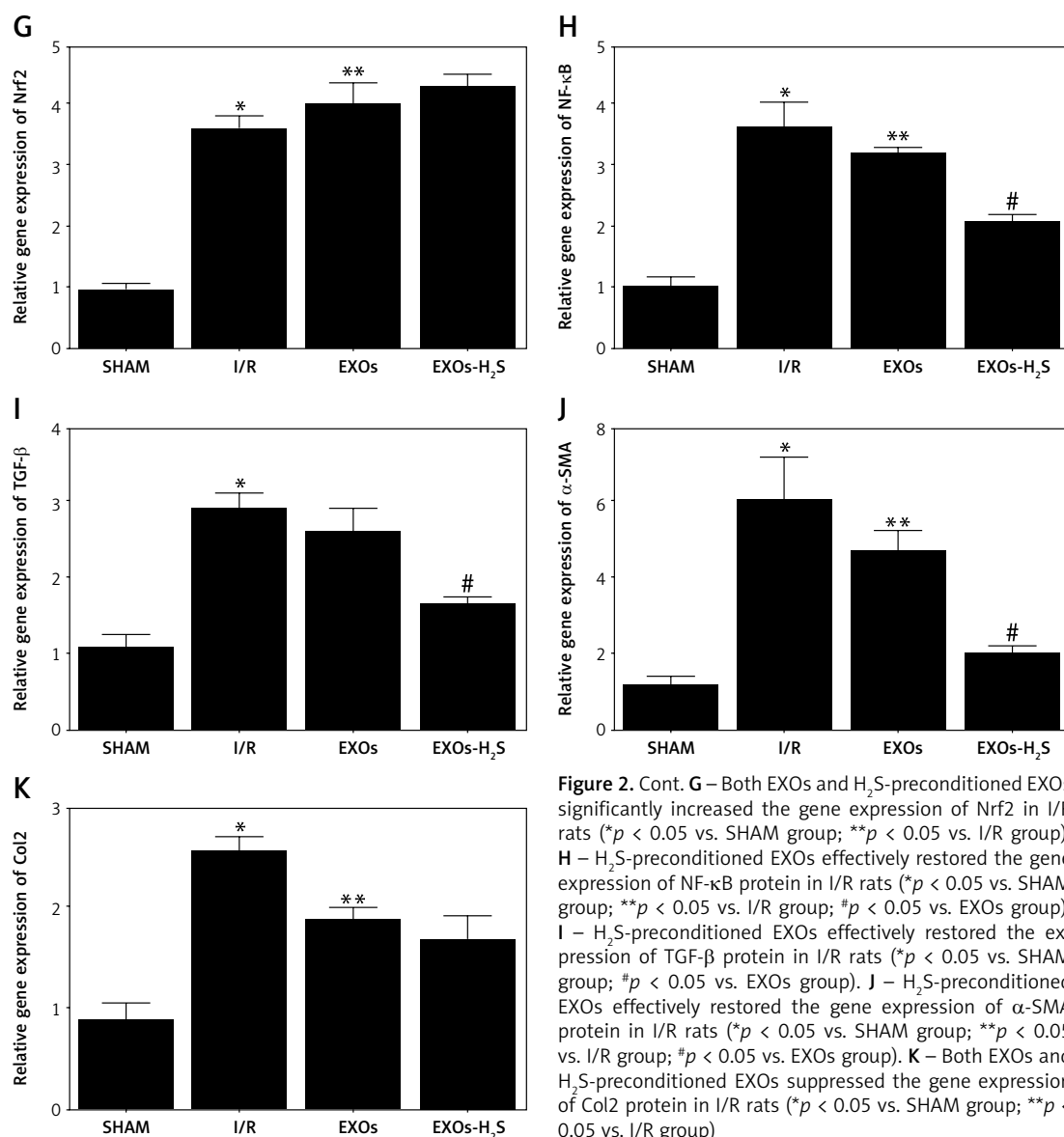


**Figure 2.** Cont. **G** – Both EXOs and H<sub>2</sub>S-preconditioned EXOs significantly increased the gene expression of Nrf2 in I/R rats (\**p* < 0.05 vs. SHAM group; \*\**p* < 0.05 vs. I/R group). **H** – H<sub>2</sub>S-preconditioned EXOs effectively restored the gene expression of NF- $\kappa$ B protein in I/R rats (\**p* < 0.05 vs. SHAM group; \*\**p* < 0.05 vs. I/R group; #*p* < 0.05 vs. EXOs group). **I** – H<sub>2</sub>S-preconditioned EXOs effectively restored the expression of TGF- $\beta$  protein in I/R rats (\**p* < 0.05 vs. SHAM group; #*p* < 0.05 vs. EXOs group). **J** – H<sub>2</sub>S-preconditioned EXOs effectively restored the gene expression of  $\alpha$ -SMA protein in I/R rats (\**p* < 0.05 vs. SHAM group; \*\**p* < 0.05 vs. I/R group; #*p* < 0.05 vs. EXOs group). **K** – Both EXOs and H<sub>2</sub>S-preconditioned EXOs suppressed the gene expression of Col2 protein in I/R rats (\**p* < 0.05 vs. SHAM group; \*\**p* < 0.05 vs. I/R group)

TGF- $\beta$  (Figure 2 D),  $\alpha$ -SMA (Figure 2 E), and Col2 (Figure 2 F) in I/R rats. Moreover, we also performed quantitative real-time PCR upon the gene expression of Nrf2 (Figure 2 G), NF- $\kappa$ B (Figure 2 H), TGF- $\beta$  (Figure 2 I),  $\alpha$ -SMA (Figure 2 J), and Col2 (Figure 2 K) in the rat models, and similar results were obtained.

#### H<sub>2</sub>S-preconditioned EXOs effectively restored the expression of IL-1 $\alpha$ , IL-6, IL-12 and TNF- $\alpha$ in I/R rats

ELISA was performed to analyze the distinct expression of IL-1 $\alpha$ , IL-6, IL-12 and TNF- $\alpha$  in I/R rat models under differential treatments. The expression of IL-1 $\alpha$ , IL-6, IL-12 and TNF- $\alpha$  was remarkably activated in the kidney of I/R rats compared with the control. EXO treatment effectively attenuated the up-regulation of IL-1 $\alpha$ , IL-6, IL-12 and TNF- $\alpha$ .

Moreover, H<sub>2</sub>S-preconditioning further decreased the elevated expression of IL-1 $\alpha$  (Figure 3 A), IL-6 (Figure 3 B), IL-12 (Figure 3 C) and TNF- $\alpha$  (Figure 3 D) in the kidney of I/R rats.

#### H<sub>2</sub>S-preconditioned EXOs effectively restored the enzymatic activities of SOD, MDA, H<sub>2</sub>O<sub>2</sub>, GST and GPx in I/R rats

Enzymatic activities of SOD, MDA, H<sub>2</sub>O<sub>2</sub>, glutathione S-transferase (GST) and GPx were evaluated in I/R rats under distinct conditions. The enzymatic activities of SOD, GST and GPx were notably suppressed in I/R rats compared with the control. EXO treatment effectively restored the suppressed activities of SOD, GST and GPx, and H<sub>2</sub>S preconditioning showed increased efficiency in restoring the enzymatic activities of SOD (Figure 4 A), GST (Figure 4 D) and GPx (Figure 4 E). However, the en-

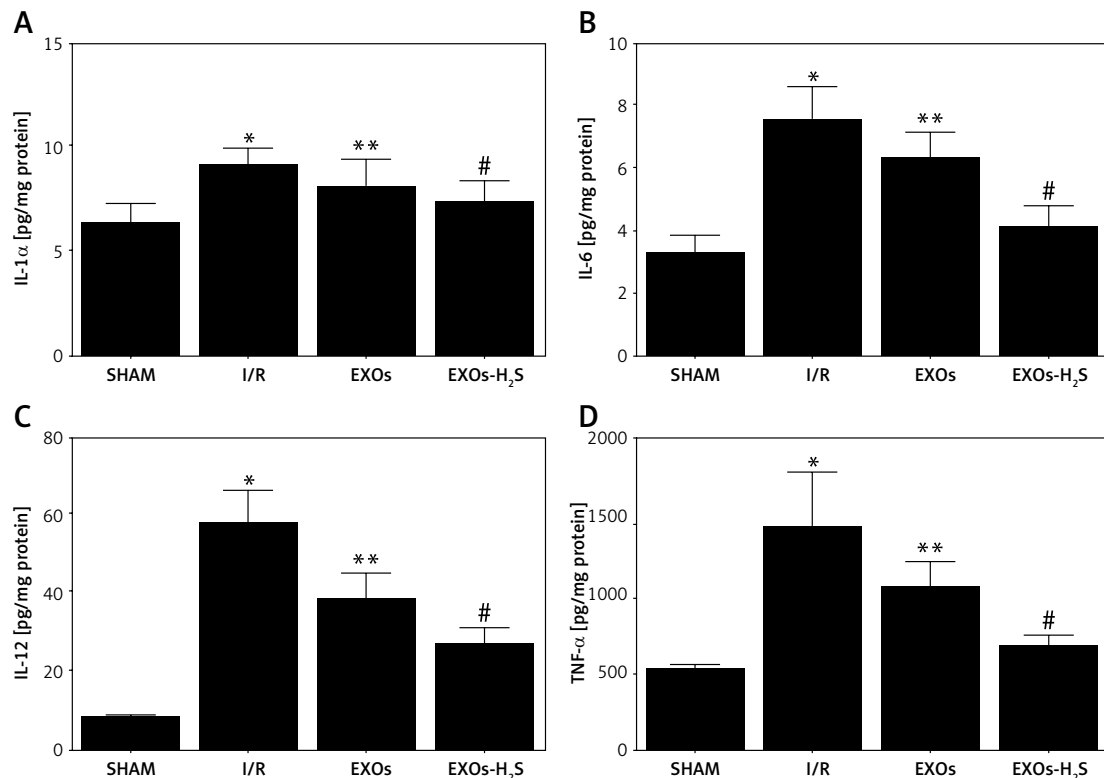


**Figure 3.** H<sub>2</sub>S-preconditioned EXOs effectively restored the expression of IL-1α, IL-6, IL-12 and TNF-α in I/R rats (\**p* < 0.05 vs. SHAM group; \*\**p* < 0.05 vs. I/R group; #*p* < 0.05 vs. EXOs group). **A** – H<sub>2</sub>S-preconditioned EXOs effectively restored the expression of IL-1α in I/R rats. **B** – H<sub>2</sub>S-preconditioned EXOs effectively restored the expression of IL-6 in I/R rats. **C** – H<sub>2</sub>S-preconditioned EXOs effectively restored the expression of IL-12 in I/R rats. **D** – v-preconditioned EXOs effectively restored the expression of TNF-α in I/R rats

zymatic activities of MDA and H<sub>2</sub>O<sub>2</sub> were notably activated in I/R rats compared with the control. EXO treatment effectively decreased the elevated activities of MDA and H<sub>2</sub>O<sub>2</sub>, and H<sub>2</sub>S preconditioning showed increased efficiency in restoring the enzymatic activities of MDA (Figure 4 B) and H<sub>2</sub>O<sub>2</sub> (Figure 4 C).

#### H<sub>2</sub>S-preconditioned EXOs effectively restored the expression of α-SMA, Col2 protein and the enzymatic activities of SOD, MDA, H<sub>2</sub>O<sub>2</sub>, GST and GPx in HK-2 H/R models

A HK-2 cell H/R model was established as described followed by EXO treatment. Western blot was performed to analyze the expression of Nrf2, α-SMA and Col2 (Figure 5 A) in HK-2 H/R models under distinct conditions. The expression of Nrf2 was notably elevated in HK-2 H/R models compared with the control. EXO treatment further increased the Nrf2 expression and H<sub>2</sub>S-preconditioned EXOs showed higher efficiency in enhancing the Nrf2 expression in HK-2 H/R models (Figure 5 B). Even though the expression of α-SMA and Col2 in HK-2 H/R models was remarkably increased, EXO treatment effectively attenuated the up-regulation of α-SMA, and Col2 in HK-2 H/R

models. Moreover, H<sub>2</sub>S preconditioning further decreased the elevated expression of α-SMA (Figure 5 C) and Col2 (Figure 5 D) in HK-2 H/R models. Moreover, we also performed quantitative real-time PCR upon the gene expression of Nrf2 (Figure 5 E), α-SMA (Figure 5 F), and Col2 (Figure 5 G) in the rat models, and similar results were obtained. The enzymatic activities of SOD, GST and GPx were notably suppressed in HK-2 H/R models compared with the control. EXOs treatment effectively restored the suppressed activities of SOD, GST and GPx, and H<sub>2</sub>S preconditioning showed higher efficiency in restoring the enzymatic activities of SOD (Figure 5 H), GST (Figure 5 K) and GPx (Figure 5 L). However, the enzymatic activities of MDA and H<sub>2</sub>O<sub>2</sub> were notably activated in HK-2 H/R models compared with the control. EXO treatment effectively decreased the elevated activities of MDA and H<sub>2</sub>O<sub>2</sub>, and H<sub>2</sub>S preconditioning showed increasing efficiency in restoring the enzymatic activities of MDA (Figure 5 I) and H<sub>2</sub>O<sub>2</sub> (Figure 5 J).

#### H<sub>2</sub>S-preconditioned EXOs effectively restored the expression of NF-κB, TGF-β, IL-1α, IL-6, IL-12 and TNF-α in THP-1 H/R models

A THP-1 cell H/R model was established as described followed by EXO treatment. Western blot



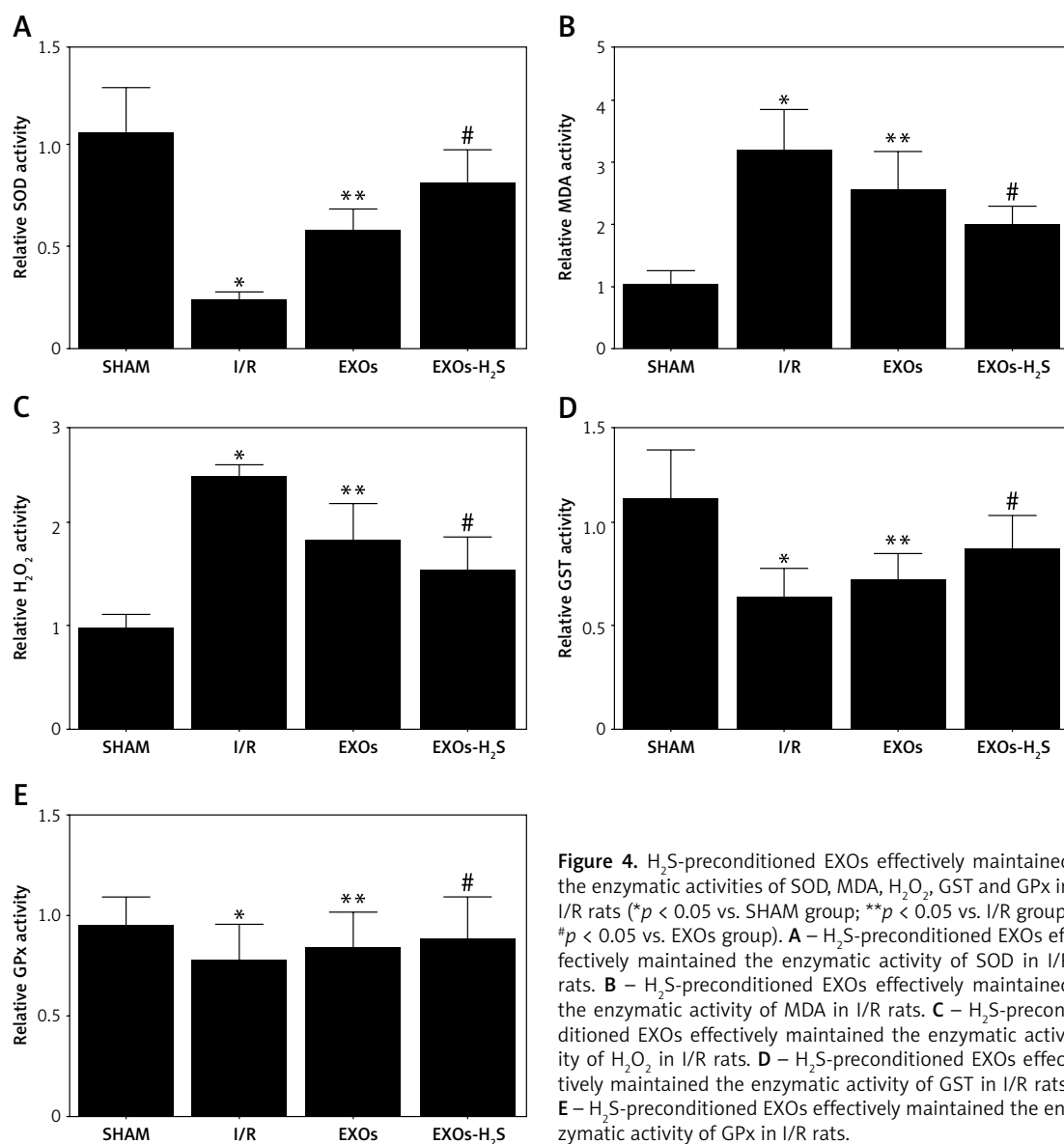


**Figure 4.** H<sub>2</sub>S-preconditioned EXOs effectively maintained the enzymatic activities of SOD, MDA, H<sub>2</sub>O<sub>2</sub>, GST and GPx in I/R rats (\**p* < 0.05 vs. SHAM group; \*\**p* < 0.05 vs. I/R group; #*p* < 0.05 vs. EXOs group). **A** – H<sub>2</sub>S-preconditioned EXOs effectively maintained the enzymatic activity of SOD in I/R rats. **B** – H<sub>2</sub>S-preconditioned EXOs effectively maintained the enzymatic activity of MDA in I/R rats. **C** – H<sub>2</sub>S-preconditioned EXOs effectively maintained the enzymatic activity of H<sub>2</sub>O<sub>2</sub> in I/R rats. **D** – H<sub>2</sub>S-preconditioned EXOs effectively maintained the enzymatic activity of GST in I/R rats. **E** – H<sub>2</sub>S-preconditioned EXOs effectively maintained the enzymatic activity of GPx in I/R rats.

was performed to analyze the expression of NF- $\kappa$ B and TGF- $\beta$  (Figure 6 A). The expression of NF- $\kappa$ B and TGF- $\beta$  in THP-1 H/R models was remarkably increased, and EXO treatment effectively attenuated the up-regulation of NF- $\kappa$ B and TGF- $\beta$  in THP-1 H/R models. Moreover, H<sub>2</sub>S preconditioning further decreased the elevated expression of NF- $\kappa$ B (Figure 6 B) and TGF- $\beta$  (Figure 6 C) in THP-1 H/R models. Also quantitative real-time PCR was performed to investigate the expression of NF- $\kappa$ B mRNA (Figure 6 D) and TGF- $\beta$  mRNA (Figure 6 E) in the cell models, showing similar results as the protein expression. ELISA was performed to analyze the distinct expression of IL-1 $\alpha$ , IL-6, IL-12 and TNF- $\alpha$  in THP-1 H/R models under differential treatments. The expression of IL-1 $\alpha$ , IL-6, IL-12 and TNF- $\alpha$  was remarkably activated in THP-1 H/R models compared with the control. EXO treatment effectively attenuated the up-regulation of IL-1 $\alpha$ ,

IL-6, IL-12 and TNF- $\alpha$ . Moreover, H<sub>2</sub>S preconditioning further decreased the elevated expression of IL-1 $\alpha$  (Figure 6 F), IL-6 (Figure 6 G), IL-12 (Figure 6 H) and TNF- $\alpha$  (Figure 6 I) in THP-1 H/R models.

## Discussion

Many surgical procedures in the kidney inevitably lead to renal IRI [26]. The end state of kidney injury caused by IRI is diagnosed based on renal fibrosis which involves glomerulosclerosis and tubulointerstitial fibrosis [29]. This type of progression to renal failure is mostly irreversible and is the main reason for the higher mortality rate of this disease [30]. A complex mixture of factors is responsible for progressive renal fibrosis, which include growth factors, reactive oxygen species, cytokines and metabolic waste [31]. In this study, administration of H<sub>2</sub>S-preconditioned exosomes

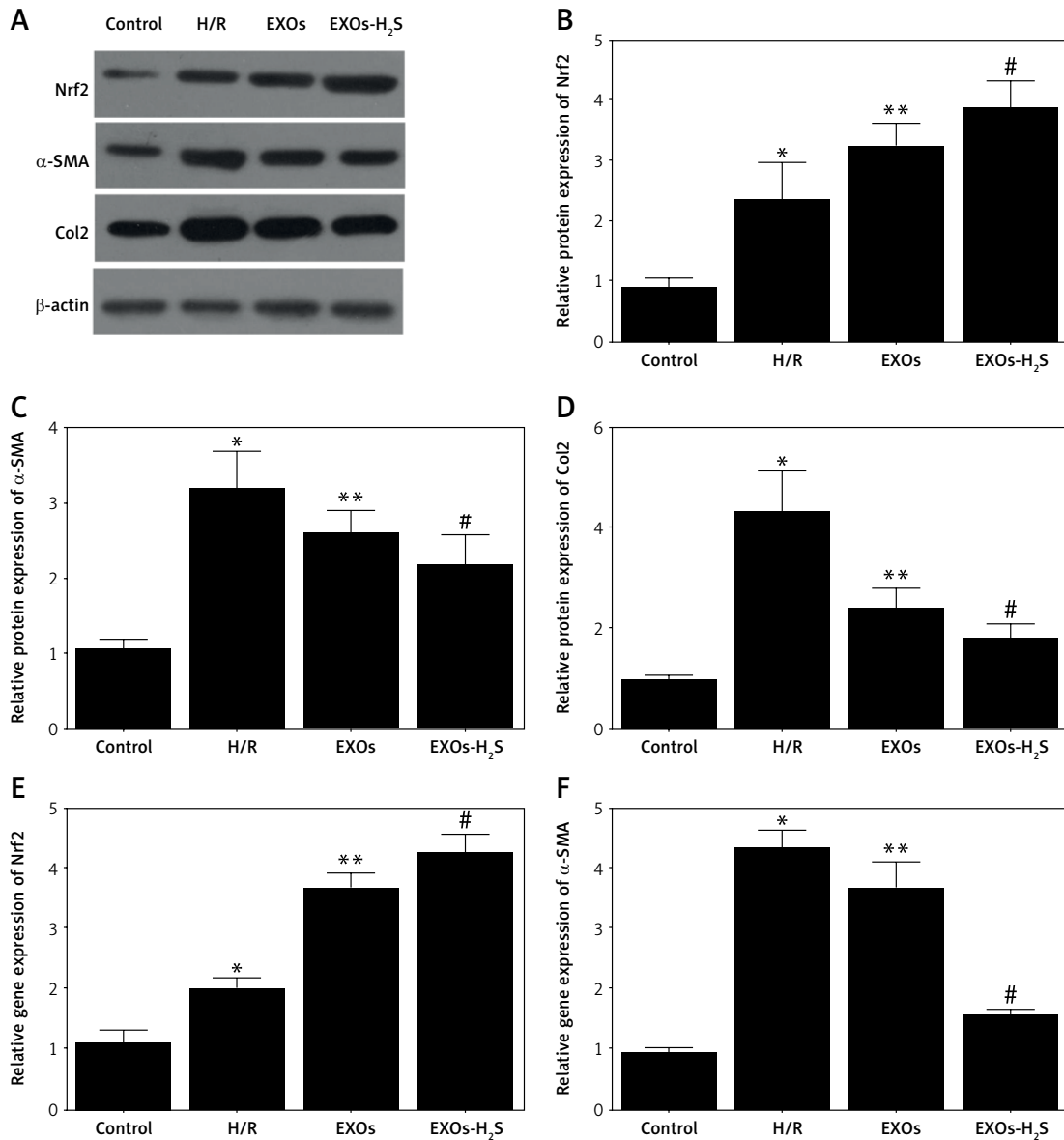


**Figure 5.** H<sub>2</sub>S-preconditioned EXOs effectively restored the expression of  $\alpha$ -SMA, Col2 protein and the enzymatic activities of SOD, MDA, H<sub>2</sub>O<sub>2</sub>, GST and GPx in HK-2 H/R models. **A** – Western blot analysis of Nrf2,  $\alpha$ -SMA, Col2 protein in HK-2 H/R models under distinct conditions. **B** – H<sub>2</sub>S-preconditioned EXOs further increased the protein expression of Nrf2 in HK-2 H/R models (\* $p$  < 0.05 vs. control group; \*\* $p$  < 0.05 vs. H/R group; # $p$  < 0.05 vs. EXOs group). **C** – H<sub>2</sub>S-preconditioned EXOs effectively restored the protein expression of  $\alpha$ -SMA protein in HK-2 H/R models (\* $p$  < 0.05 vs. control group; \*\* $p$  < 0.05 vs. H/R group; # $p$  < 0.05 vs. EXOs group). **D** – H<sub>2</sub>S-preconditioned EXOs effectively restored the protein expression of Col2 protein in HK-2 H/R models (\* $p$  < 0.05 vs. control group; \*\* $p$  < 0.05 vs. H/R group; # $p$  < 0.05 vs. EXOs group). **E** – H<sub>2</sub>S-preconditioned EXOs further increased the gene expression of Nrf2 in HK-2 H/R models (\* $p$  < 0.05 vs. control group; \*\* $p$  < 0.05 vs. H/R group; # $p$  < 0.05 vs. EXOs group). **F** – H<sub>2</sub>S-preconditioned EXOs effectively restored the gene expression of  $\alpha$ -SMA protein in HK-2 H/R models (\* $p$  < 0.05 vs. control group; \*\* $p$  < 0.05 vs. H/R group; # $p$  < 0.05 vs. EXOs group)

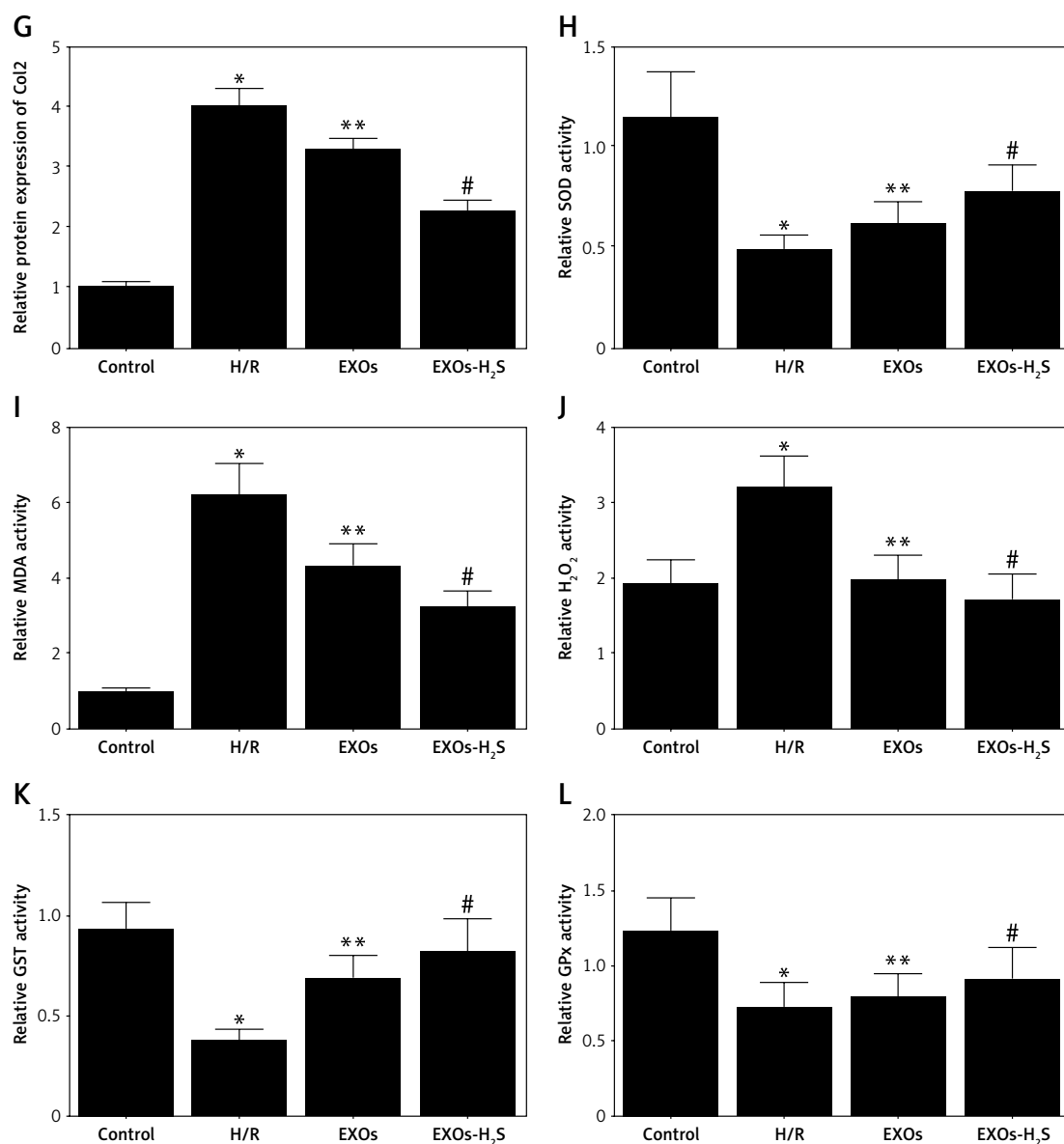


**Figure 5.** Cont. **G** – H<sub>2</sub>S-preconditioned EXOs effectively restored the gene expression of Col2 protein in HK-2 H/R models (\**p* < 0.05 vs. control group; \*\**p* < 0.05 vs. H/R group; #*p* < 0.05 vs. EXOs group). **H** – H<sub>2</sub>S-preconditioned EXOs effectively maintained the enzymatic activities of SOD in HK-2 H/R models (\**p* < 0.05 vs. control group; \*\**p* < 0.05 vs. H/R group; #*p* < 0.05 vs. EXOs group). **I** – H<sub>2</sub>S-preconditioned EXOs effectively maintained the enzymatic activities of MDA in HK-2 H/R models (\**p* < 0.05 vs. control group; \*\**p* < 0.05 vs. H/R group; #*p* < 0.05 vs. EXOs group). **J** – H<sub>2</sub>S-preconditioned EXOs effectively maintained the enzymatic activities of H<sub>2</sub>O<sub>2</sub> in HK-2 H/R models (\**p* < 0.05 vs. control group; \*\**p* < 0.05 vs. H/R group; #*p* < 0.05 vs. EXOs group). **K** – H<sub>2</sub>S-preconditioned EXOs effectively maintained the enzymatic activities of GST in HK-2 H/R models (\**p* < 0.05 vs. control group; \*\**p* < 0.05 vs. H/R group; #*p* < 0.05 vs. EXOs group). **L** – H<sub>2</sub>S-preconditioned EXOs effectively maintained the enzymatic activities of GPx in HK-2 H/R models (\**p* < 0.05 vs. control group; \*\**p* < 0.05 vs. H/R group; #*p* < 0.05 vs. EXOs group)

successfully restored the renal function in I/R rat models. Additionally, the authors also performed Western blot analysis to correlate expression of Nrf2, NF- $\kappa$ B, TGF- $\beta$ ,  $\alpha$ -SMA, and Col2 with treatment of H<sub>2</sub>S pretreated or untreated exosomes in I/R rat and cellular models.

In the past few decades, application of stem cell therapy has become popular as an adjuvant strategy to treat I/R diseases [32]. However, the

exact mechanism of action remains elusive. Another study showed that administration of human adipose (hAD) derived mesenchymal stem cells in I/R mice provided protection against acute and chronic renal injury. The therapy decreased penetration of inflammatory cells as well as enhancing activity of IL-10, which suggested that the therapy altered the microenvironment of the kidney cells and the result of the study revealed that hAD-MSC

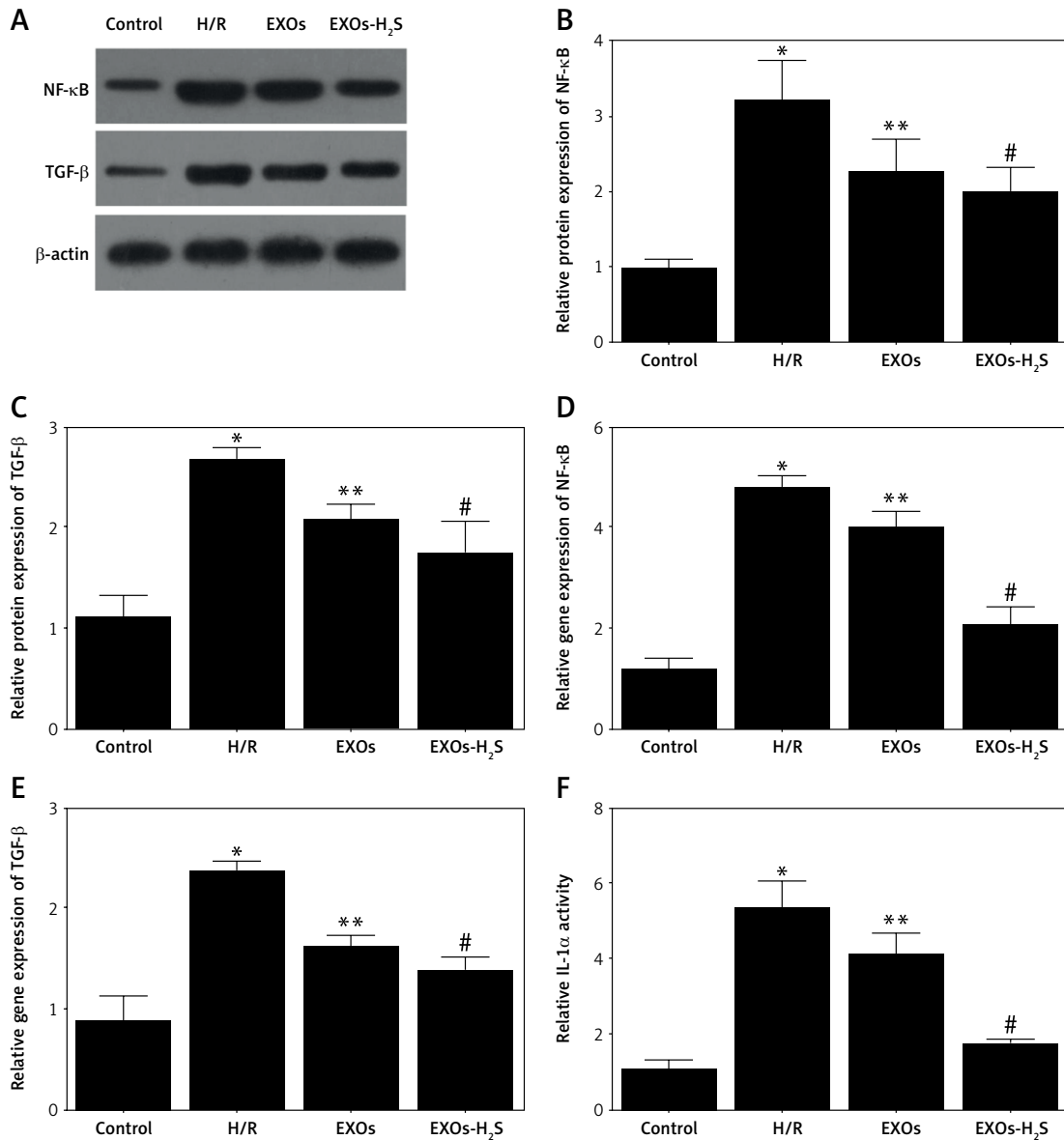


**Figure 6.** H<sub>2</sub>S-preconditioned EXOs effectively restored the expression of NF-κB, TGF-β, IL-1α, IL-6, IL-12 and TNF-α in THP-1 H/R models. **A** – Western blot analysis of NF-κB, TGF-β protein in THP-1 H/R models under distinct conditions. **B** – H<sub>2</sub>S-preconditioned EXOs effectively restored the expression of NF-κB protein in THP-1 H/R models (\**p* < 0.05 vs. control group; \*\**p* < 0.05 vs. H/R group; #*p* < 0.05 vs. EXOs group). **C** – H<sub>2</sub>S-preconditioned EXOs effectively restored the expression of TGF-β protein in THP-1 H/R models (\**p* < 0.05 vs. control group; \*\**p* < 0.05 vs. H/R group; #*p* < 0.05 vs. EXOs group). **D** – H<sub>2</sub>S-preconditioned EXOs effectively restored the expression of NF-κB mRNA in THP-1 H/R models (\**p* < 0.05 vs. control group; \*\**p* < 0.05 vs. H/R group; #*p* < 0.05 vs. EXOs group). **E** – H<sub>2</sub>S-preconditioned EXOs effectively restored the expression of TGF-β mRNA in THP-1 H/R models (\**p* < 0.05 vs. control group; \*\**p* < 0.05 vs. H/R group; #*p* < 0.05 vs. EXOs group). **F** – H<sub>2</sub>S-preconditioned EXOs effectively restored the expression of IL-1α in THP-1 H/R models (\**p* < 0.05 vs. control group; \*\**p* < 0.05 vs. H/R group; #*p* < 0.05 vs. EXOs group)

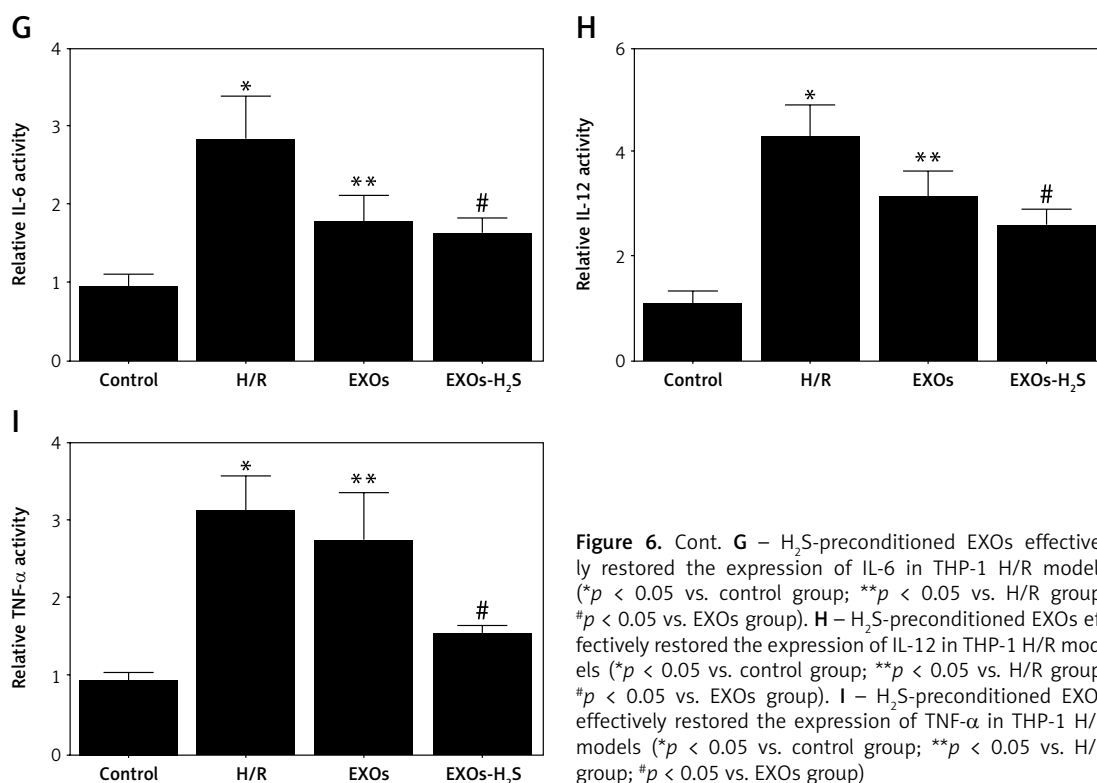


**Figure 6.** Cont. **G** – H<sub>2</sub>S-preconditioned EXOs effectively restored the expression of IL-6 in THP-1 H/R models (\* $p$  < 0.05 vs. control group; \*\* $p$  < 0.05 vs. H/R group; # $p$  < 0.05 vs. EXOs group). **H** – H<sub>2</sub>S-preconditioned EXOs effectively restored the expression of IL-12 in THP-1 H/R models (\* $p$  < 0.05 vs. control group; \*\* $p$  < 0.05 vs. H/R group; # $p$  < 0.05 vs. EXOs group). **I** – H<sub>2</sub>S-preconditioned EXOs effectively restored the expression of TNF- $\alpha$  in THP-1 H/R models (\* $p$  < 0.05 vs. control group; \*\* $p$  < 0.05 vs. H/R group; # $p$  < 0.05 vs. EXOs group)

therapy reduced chronic renal injury and fibrosis. Other pathophysiological conditions, such as unilateral urethral obstruction and vitamin B9 induced kidney fibrosis, also improved following hAD-MSC therapy [33, 34].

Many researchers have shown that H<sub>2</sub>S treatment has protective effects against several pathophysiological processes as well as various types of renal ischemia/reperfusion injury [35, 36]. Previous research also proved that H<sub>2</sub>S treatment protected against cold IRI for a longer duration, as well as against warm IRI for a shorter period [20, 37]. Another study revealed that H<sub>2</sub>S treatment provided both short-term and long-term renal protection against warm IRI. It has been suggested that the regulation of iNOS activation-induced NO release is closely related to the mechanisms of H<sub>2</sub>S-related kidney protection [38, 39]. Apart from NO, other gasotransmitter such as CO can interact with NO and H<sub>2</sub>S [40]. For example, H<sub>2</sub>S was significantly minimized in the presence of CO inhibitor [41]. Previous studies have shown that a H<sub>2</sub>S donor could suppress the overproduction of NO, while simultaneously inhibiting the level of pro-inflammatory mediators such as IL-1 $\beta$ , IL-6, TNF- $\alpha$ , which indicated the potential positive effect on inflammation resulting from the crosstalk between H<sub>2</sub>S and NO [42]. Moreover, H<sub>2</sub>S therapy was found to successfully restore NO concentration and eNOS functions in individuals with IR injury [43], and NOS isoforms can reduce kidney damage [44]. Moreover, it was also reported that the T allele of

the eNOS gene G894T polymorphism is associated with hypertension in women [45].

It has been shown that levels of Nrf2 protein in the renal tissue after fasting are not involved in protection against oxidative stress caused by IRI [46]. The study also suggested that mitochondrial pathways are also involved in protective effects of fasting in IRI [47]. The results showed that fasting alleviates dysregulation in oxygen consumption, action potential in mitochondrial membrane, structure of mitochondria and balance of protein levels between mitochondria and the nucleus. Also, fasting also helped to lower the risk of fibrosis in the injured kidney. In this study, we performed ELISA to measure the expression levels of IL-1 $\alpha$ , IL-6, IL-12 and TNF- $\alpha$  in I/R rat and cellular models under specific conditions. Moreover, the H<sub>2</sub>S-pretreated exosomes successfully improved the expression levels of IL-1 $\alpha$ , IL-6, IL-12 and TNF- $\alpha$ . Meanwhile, we also evaluated expression of NF- $\kappa$ B and H<sub>2</sub>S-preconditioned EXO restored elevated expression of NF- $\kappa$ B caused by IRI. Several studies have shown that NF- $\kappa$ B is an important transcription factor involved in inflammatory regulation [48]. The NF- $\kappa$ B is a key player in different types of cellular damage and inflammation caused by chemical hypoxia, doxorubicin and LPS [49, 50].

Injury to cells and organs caused during reperfusion are mainly due to ROS production [51]. According to the previous findings H<sub>2</sub>S changes the conformation of Keap1, therefore releasing the bound



Nrf2, which subsequently protects the protein from proteasomal degradation [52, 53]. The Nrf2 accumulated in the cytoplasm translocated into the nucleus, where it was phosphorylated to promote transcription of antioxidant genes [54, 55]. In this study, we evaluated the enzymatic activities of SOD, MDA,  $H_2O_2$ , GST and GPx in I/R rat and cellular models under distinct conditions.  $H_2S$ -preconditioned EXOs effectively restored the enzymatic activities of SOD, MDA,  $H_2O_2$ , GST and GPx. The results of this study shed light on the clinical use of MSCs in the treatment and prevention of development of fibrosis following renal ischemia reperfusion injury. Furthermore, pre-conditioning of MSCs with  $H_2S$  will further promote the therapeutic effect of MSCs. In addition, the level of  $H_2S$  could be a biomarker for the prognosis and risk of fibrosis following renal reperfusion injury.

In conclusion, this study utilized I/R rats to demonstrate that the effect of  $H_2S$ -preconditioned exosomes in suppressing inflammation and ROS generation was better than that of unconditioned exosomes. To be specific, exosomes, especially  $H_2S$ -preconditioned exosomes, could not only reduce the expression of NF- $\kappa$ B and the downstream inflammatory responses, but also promote the expression of Nrf2 and inhibit ROS generation, which explained the molecular mechanism underlying the protective effect of  $H_2S$ -preconditioned exosomes on renal I/R associated fibrosis.

## Acknowledgments

This research was supported by Natural Science Foundation of Ningxia Province of China (2022AAC03170) and Key Cultivation Nurture Discipline Project of the Second Phase of First-class End Discipline Construction in Ningxia Universities (NYHLZD06).

## Conflict of interest

The authors declare no conflict of interest.

## References

- Wang X, Liu J, Yin W, et al. miR-218 expressed in endothelial progenitor cells contributes to the development and repair of the kidney microvasculature. *Am J Pathol* 2020; 190: 642-59.
- Fine LG, Norman JT. Chronic hypoxia as a mechanism of progression of chronic kidney diseases: from hypothesis to novel therapeutics. *Kidney Int* 2008; 74: 867-72.
- Yan W, Lin C, Guo Y, et al. N-cadherin overexpression mobilizes the protective effects of mesenchymal stromal cells against ischemic heart injury through a beta-catenin-dependent manner. *Circ Res* 2020; 126: 857-74.
- Basile DP. The endothelial cell in ischemic acute kidney injury: implications for acute and chronic function. *Kidney Int* 2007; 72: 151-6.
- Kapitsinou PP, Sano H, Michael M, et al. Endothelial HIF-2 mediates protection and recovery from ischemic kidney injury. *J Clin Invest* 2014; 124: 2396-409.
- Zuk A, Bonventre JV. Acute kidney injury. *Annu Rev Med* 2016; 67: 293-307.
- Yang C, Chen Z, Yu H, Liu X. Inhibition of disruptor of telomeric silencing 1-like alleviated renal ischemia and reperfusion injury-induced fibrosis by blocking PI3K/AKT-mediated oxidative stress. *Drug Des Devel Ther* 2019; 13: 4375-87.
- Lee RH, Pulin AA, Seo MJ, et al. Intravenous hMSCs improve myocardial infarction in mice because cells embolized in lung are activated to secrete the anti-inflammatory protein TSG-6. *Cell Stem Cell* 2009; 5: 54-63.
- Chen J, Li Y, Wang L, et al. Therapeutic benefit of intravenous administration of bone marrow stromal cells after cerebral ischemia in rats. *Stroke* 2001; 32: 1005-11.
- Kopen GC, Prockop DJ, Phinney DG. Marrow stromal cells migrate throughout forebrain and cerebellum, and they differentiate into astrocytes after injection into neonatal mouse brains. *Proc Natl Acad Sci USA* 1999; 96: 10711-6.
- Jiang W, Ma A, Wang T, et al. Intravenous transplantation of mesenchymal stem cells improves cardiac performance after acute myocardial ischemia in female rats. *Transpl Int* 2006; 19: 570-80.
- Colombo M, Raposo G, Thery C. Biogenesis, secretion, and intercellular interactions of exosomes and other extracellular vesicles. *Annu Rev Cell Dev Biol* 2014; 30: 255-89.
- Thery C, Zitvogel L, Amigorena S. Exosomes: composition, biogenesis and function. *Nat Rev Immunol* 2002; 2: 569-79.
- Valadi H, Ekstrom K, Bossios A, Sjostrand M, Lee JJ, Lotvall JO. Exosome-mediated transfer of mRNAs and microRNAs is a novel mechanism of genetic exchange between cells. *Nat Cell Biol* 2007; 9: 654-9.
- Phinney DG, Di Giuseppe M, Njah J, et al. Mesenchymal stem cells use extracellular vesicles to outsource mitophagy and shuttle microRNAs. *Nat Commun* 2015; 6: 8472.
- Wang R. Two's company, three's a crowd: can  $H_2S$  be the third endogenous gaseous transmitter? *FASEB J* 2002; 16: 1792-8.
- Szabo C. Hydrogen sulphide and its therapeutic potential. *Nat Rev Drug Discov* 2007; 6: 917-35.
- Li Z, Wang Y, Xie Y, Yang Z, Zhang T. Protective effects of exogenous hydrogen sulfide on neurons of hippocampus in a rat model of brain ischemia. *Neurochem Res* 2011; 36: 1840-9.
- Liu Y, Kalogeris T, Wang M, et al. Hydrogen sulfide preconditioning or neutrophil depletion attenuates ischemia-reperfusion-induced mitochondrial dysfunction in rat small intestine. *Am J Physiol Gastrointest Liver Physiol* 2012; 302: G44-54.
- Zhu JX, Kalbfleisch M, Yang YX, et al. Detrimental effects of prolonged warm renal ischaemia-reperfusion injury are abrogated by supplemental hydrogen sulphide: an analysis using real-time intravital microscopy and polymerase chain reaction. *BJU Int* 2012; 110: E1218-27.
- Wang M, Xu H, Li Y, et al. Exogenous bone marrow derived-putative endothelial progenitor cells attenuate ischemia reperfusion-induced vascular injury and renal fibrosis in mice dependent on pericytes. *Theranostics* 2020; 10: 12144-57.
- Bos EM, Wang R, Snijder PM, et al. Cystathionine gamma-lyase protects against renal ischemia/reperfusion

- by modulating oxidative stress. *J Am Soc Nephrol* 2013; 24: 759-70.
23. Ishiuchi N, Nakashima A, Doi S, et al. Hypoxia-preconditioned mesenchymal stem cells prevent renal fibrosis and inflammation in ischemia-reperfusion rats. *Stem Cell Res Ther* 2020; 11: 130.
24. Du Y, Liu XH, Zhu HC, et al. Hydrogen sulfide treatment protects against renal ischemia-reperfusion injury via induction of heat shock proteins in rats. *Iran J Basic Med Sci* 2019; 22: 99-105.
25. Ling Q, Yu X, Wang T, Wang SG, Ye ZQ, Liu JH. Roles of the exogenous H<sub>2</sub>S-mediated SR-A signaling pathway in renal ischemia/ reperfusion injury in regulating endoplasmic reticulum stress-induced autophagy in a rat model. *Cell Physiol Biochem* 2017; 41: 2461-74.
26. Ponticelli C. Ischaemia-reperfusion injury: a major protagonist in kidney transplantation. *Nephrol Dial Transplant* 2014; 29: 1134-40.
27. Xie X, Sun A, Zhu W, et al. Transplantation of mesenchymal stem cells preconditioned with hydrogen sulfide enhances repair of myocardial infarction in rats. *Tohoku J Exp Med* 2012; 226: 29-36.
28. Kaide JI, Zhang F, Wei Y, et al. Carbon monoxide of vascular origin attenuates the sensitivity of renal arterial vessels to vasoconstrictors. *J Clin Invest* 2001; 107: 1163-71.
29. Fan H, Yang HC, You L, Wang YY, He WJ, Hao CM. The histone deacetylase, SIRT1, contributes to the resistance of young mice to ischemia/reperfusion-induced acute kidney injury. *Kidney Int* 2013; 83: 404-13.
30. Webster AC, Nagler EV, Morton RL, Masson P. Chronic kidney disease. *Lancet* 2017; 389: 1238-52.
31. Lan HY. Diverse roles of TGF-beta/Smads in renal fibrosis and inflammation. *Int J Biol Sci* 2011; 7: 1056-67.
32. de Couto G, Liu W, Tseliou E, et al. Macrophages mediate cardioprotective cellular postconditioning in acute myocardial infarction. *J Clin Invest* 2015; 125: 3147-62.
33. Huuskies BM, Wise AF, Cox AJ, et al. Combination therapy of mesenchymal stem cells and serelaxin effectively attenuates renal fibrosis in obstructive nephropathy. *FASEB J* 2015; 29: 540-53.
34. Burgos-Silva M, Semedo-Kuriki P, Donizetti-Oliveira C, et al. Adipose tissue-derived stem cells reduce acute and chronic kidney damage in mice. *PLoS One* 2015; 10: e0142183.
35. Tripatara P, Patel NS, Collino M, et al. Generation of endogenous hydrogen sulfide by cystathionine gamma-lyase limits renal ischemia/reperfusion injury and dysfunction. *Lab Invest* 2008; 88: 1038-1048.
36. Hunter JP, Hosgood SA, Patel M, Rose R, Read K, Nicholson ML. Effects of hydrogen sulphide in an experimental model of renal ischaemia-reperfusion injury. *Br J Surg* 2012; 99: 1665-71.
37. Lobb I, Mok A, Lan Z, Liu W, Garcia B, Sener A. Supplemental hydrogen sulphide protects transplant kidney function and prolongs recipient survival after prolonged cold ischaemia-reperfusion injury by mitigating renal graft apoptosis and inflammation. *BJU Int* 2012; 110: E1187-95.
38. Tripatara P, Patel NS, Collino M, et al. Generation of endogenous hydrogen sulfide by cystathionine gamma-lyase limits renal ischemia/reperfusion injury and dysfunction. *Lab Invest* 2008; 88: 1038-48.
39. Oh GS, Pae HO, Lee BS, et al. Hydrogen sulfide inhibits nitric oxide production and nuclear factor-kappaB via heme oxygenase-1 expression in RAW264.7 macrophages stimulated with lipopolysaccharide. *Free Radic Biol Med* 2006; 41: 106-19.
40. Pae HO, Lee YC, Jo EK, Chung HT. Subtle interplay of endogenous bioactive gases (NO, CO and H(2)S) in inflammation. *Arch Pharm Res* 2009; 32: 1155-62.
41. Aziz NM, Elbassuoni EA, Kamel MY, Ahmed SM. Hydrogen sulfide renal protective effects: possible link between hydrogen sulfide and endogenous carbon monoxide in a rat model of renal injury. *Cell Stress Chaperones* 2020; 25: 211-21.
42. Hua W, Chen Q, Gong F, Xie C, Zhou S, Gao L. Cardioprotection of H<sub>2</sub>S by downregulating iNOS and upregulating HO-1 expression in mice with CVB3-induced myocarditis. *Life Sci* 2013; 93: 949-54.
43. King AL, Polhemus DJ, Bhushan S, et al. Hydrogen sulfide cytoprotective signaling is endothelial nitric oxide synthase-nitric oxide dependent. *Proc Natl Acad Sci USA* 2014; 111: 3182-7.
44. Shirazi MK, Azarnezhad A, Abazari MF, et al. The role of nitric oxide signaling in renoprotective effects of hydrogen sulfide against chronic kidney disease in rats: involvement of oxidative stress, autophagy and apoptosis. *J Cell Physiol* 2019; 234: 11411-23.
45. Neto ABL, Farias MCO, Vasconcelos NBR, Xavier AF Jr, Assunção ML, Ferreira HS. Prevalence of endothelial nitric oxide synthase (eNOS) gene G894T polymorphism and its association with hypertension: a population-based study with Brazilian women. *Arch Med Sci Atheroscler Dis* 2019; 4: e63-73.
46. Kulkarni SR, Donepudi AC, Xu J, et al. Fasting induces nuclear factor E2-related factor 2 and ATP-binding Cassette transporters via protein kinase A and Sirtuin-1 in mouse and human. *Antioxid Redox Signal* 2014; 20: 15-30.
47. Menezes-Filho SL, Amigo I, Prado FM, et al. Caloric restriction protects livers from ischemia/reperfusion damage by preventing Ca(2+)-induced mitochondrial permeability transition. *Free Radic Biol Med* 2017; 110: 219-27.
48. Barnes PJ, Karin M. Nuclear factor-kappaB: a pivotal transcription factor in chronic inflammatory diseases. *N Engl J Med* 1997; 336: 1066-71.
49. Hu LF, Wong PT, Moore PK, Bian JS. Hydrogen sulfide attenuates lipopolysaccharide-induced inflammation by inhibition of p38 mitogen-activated protein kinase in microglia. *J Neurochem* 2007; 100: 1121-8.
50. Yang C, Yang Z, Zhang M, et al. Hydrogen sulfide protects against chemical hypoxia-induced cytotoxicity and inflammation in HaCaT cells through inhibition of ROS/NF-kappaB/COX-2 pathway. *PLoS One* 2011; 6: e21971.
51. Neri M, Riezzo I, Pascale N, Pomara C, Turillazzi E. Ischemia/reperfusion injury following acute myocardial infarction: a critical issue for clinicians and forensic pathologists. *Mediators Inflamm* 2017; 2017: 7018393.
52. Yang G, Zhao K, Ju Y, et al. Hydrogen sulfide protects against cellular senescence via S-sulphydration of Keap1 and activation of Nrf2. *Antioxid Redox Signal* 2013; 18: 1906-19.
53. Hourihan JM, Kenna JG, Hayes JD. The gasotransmitter hydrogen sulfide induces nrf2-target genes by inactivating the Keap1 ubiquitin ligase substrate adaptor through formation of a disulfide bond between Cys-226 and Cys-613. *Antioxid Redox Signal* 2013; 19: 465-81.
54. Ma Q. Role of Nrf2 in oxidative stress and toxicity. *Annu Rev Pharmacol Toxicol* 2013; 53: 401-26.
55. Corsello T, Komaravelli N, Casola A. Role of hydrogen sulfide in NRF2- and sirtuin-dependent maintenance of cellular redox balance. *Antioxidants (Basel)* 2018; 7: 129.